Multi-modality diagnostic assessment in interventional cardiology

Pyxaras, S.

Chapter 7

Invasive Assessment Of Coronary Artery Disease

This chapter was adapted from:
Invasive Assessment Of Coronary Artery Disease
Stylianos A. Pyxaras, William Wijns, Johan HC Reiber, Jeroen J. Bax
Journal of Nuclear Cardiology
Epub Ahead of Print

ABSTRACT

Coronary artery disease is associated to high mortality and morbidity rates and an accurate diagnostic assessment during heart catheterization has a fundamental role in prognostic stratification and treatment choices. Coronary angiography has been integrated by intravascular imaging modalities, namely intravascular ultrasound and optical coherence tomography, which allow the precise quantification of the atherosclerotic burden of coronary arteries. The hemodynamic relevance of a given coronary stenosis can be assessed using stress or resting indexes: fractional flow reserve and instantaneous wave-free ratio are both coronary flow surrogates, used to guide percutaneous coronary interventions. This review summarizes the current state-of-the-art of invasive diagnostic methods during heart catheterization and highlights the potential role that an integration of anatomical and functional information enables.

INTRODUCTION

Ischemic heart disease remains the first cause of death worldwide and careful diagnostic assessment is key to identify pathophysiological entities of coronary artery disease (CAD), quantify the extension of epicardial vessel atherosclerosis and allow an efficient prognostic stratification for the individual patient. Furthermore, the possibility to treat the patient during the same heart catheterization session with percutaneous coronary intervention (PCI) requires real-time procedural guidance. Currently available technologies allow a detailed assessment of CAD in the heart catheterization laboratory. On the one hand, the anatomical description of extended segments of the coronary tree is nowadays feasible by the use of intravascular ultrasound (IVUS) and optical coherence tomography (OCT), two techniques using different physical principles (ultrasound and near-infrared light transmission, respectively) to assess the different coronary wall components in cross-sectional and longitudinal viewing modalities, allowing on-site tissue characterization and plaque identification (1,2). On the other hand, the use of fractional flow reserve (FFR) permits to identify the ischemic potential of a given epicardial stenosis and has an additive prognostic impact to the coronary angiographic assessment, conventionally used as a roadmap for the invasive assessment of CAD (3,4).

In this comprehensive review of the currently available invasive imaging techniques to assess CAD, we focus on potential daily-practice implications of an integrative anatomical-hemodynamic approach.

ANATOMICAL ASSESMENT

Coronary angiography

The visualization of the coronary tree using contrast media injections and different radiographic projections remains the road map upon which the invasive anatomical assessment in the catheterization laboratory is based. Coronary artery disease diagnosis is up to date based on the qualitative (visual) anatomical assessment of coronary angiography used as reference standard (5). Concerns regarding the reliability of such an approach, even by experienced operators, have been raised, considering the phenomenon of "stenosis inflation" that causes operators to assess a diameter stenosis approximately 20% higher than the one measured by quantitative coronary angiography (QCA) (6). The latter has been developed in parallel as an objective tool of quantification of the coronary "luminogram", using automatic edge detection algorithms to determine the vessel contours by assessing brightness along scan lines perpendicular to the vessel center (*centerline*) (7). For a given stenosis, an end-diastolic frame of the angiogram is selected and the angiographic projection with the most severe degree of stenosis, minimal foreshortening and branch overlap is assessed (***Figure 1***). Quantitative coronary angiography has a proven potential to improve coronary stenosis assessment, by

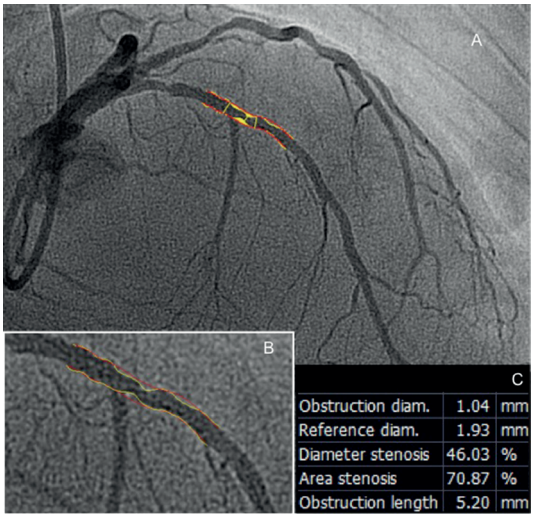

Figure 1. Quantitative assessment of coronary angiography.
Panel A: Quantitative coronary angiogiography (QCA) of a severe mid-LAD lesion; the red lines indicate the automatically detected reference vessel diameter (RVD) of the analysed coronary segment; the yellow lines indicate the vessel lumen.
Panel B: Zoomed image of the analysed segment.
Panel C: Output of the QCA analysis – obstruction diameter (corrresponding to minimal luminal diameter – MLD), RVD, diameter stenosis, area stenosis, and obstruction length.
LAD: left anterior descending artery; MLD: minimal luminal diameter; QCA: quantitative coronary angiography; RVD: reference vessel diameter.

significantly reducing errors made by operators qualitative (visual) assessment (8). The need of a systematic approach on quantitative angiographic assessment emerges particularly in complex coronary lesions, such as bifurcations, where dedicated QCA algorithms have been used (***Figure 2)*** (9). The use of specific bifurcation algorithms can positively impact the accuracy of result interpretation in trials assessing bifurcation PCI (10). In an attempt to overcome the limitations deriving from a two-dimensional assessment of a three-dimensional entity such as an epicardial vessel, new tools have been recently developed. The three-dimensional reconstruction of coronary segments using two different non-orthogonal angiographic projections is today feasible with the use of dedicated software and allows stenosis quantification in an analogue manner (3D-QCA), but perhaps higher accuracy (***Figure 3***) (11).

Intravascular ultrasound (IVUS)

Intravascular ultrasound is based on tissue-mediated sound wave reflection and image acquisition using piezoelectric transducers (12). Two different types of IVUS technologies are available for clinical use: the solid-state electronic phased array transducer and the mechanical single-element rotating transducer. Nowadays IVUS remains an essential tool in the catheterization laboratory, since it offers unique insights on qualitative and quantitative lesion assessment, as well as PCI-guidance (identifying entities such as stent malapposition, underexpansion, position of guidewires, false vs. real coronary lumen, position of side-branches). This latter is of outmost importance for complicated procedures, namely left main (LM) interventions and chronic total occlusions (CTOs). Accordingly, IVUS should be performed from both the left anterior descending and left circumflex coronary arteries to define the minimal lumen area (MLA) within the LM and to accurately assess disease at the left anterior descending and left circumflex ostia (13,14). In clinical practice, the MLA cut-off

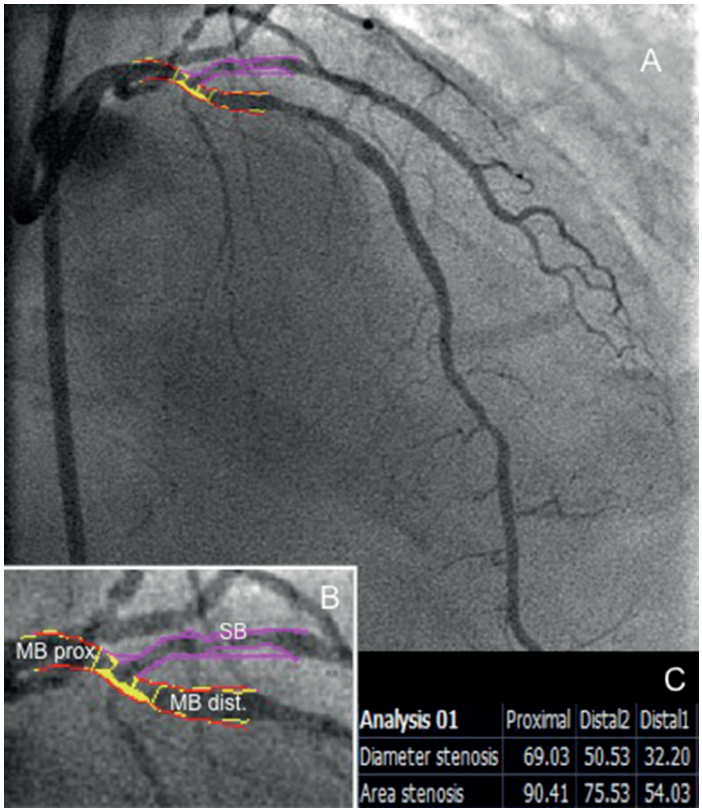

Figure 2. Quantitative coronary analysis of a bifurcation lesion with dedicated QCA-software.
Panel A: Overview of QCA of a proximal LAD – D1 bifurcation lesion; the red lines indicate the automatically detected reference vessel diameter (RVD) of the main branch (MB); the yellow lines indicate the vessel lumen of the MB; the purple lines show both RVD and vessel lumen of the side-branch (SB).
Panel B: Zoomed image of the analysed bifurcation; MB prox. indicates the proximal main branch, MB dist. indicates the distal main branch, SB shows the side branch.
Panel C: Output of the bifurcation-QCA analysis: diameter stenosis and area stenosis are given for MB prox. (here indicated as "Proximal"), MB dist. (here indicated as "Distal1"), and SB (here indicated as "Distal2").
D1: first diagonal branch; LAD: left anterior descending artery; MB: main branch; MB dist.: distal main branch; MB prox.: dproximal main branch; QCA: quantitative coronary angiography; RVD: reference vessel diameter; SB: side branch.

of 6.0 mm^2 for LM was associated with long-term clinical outcomes similar to an FFR cut-off value of 0.80 and has been used as normality-abnormality threshold (***Figure 4, panels A and B***) (15-17). Likewise, CTO-recanalization procedures may benefit from IVUS guidance to facilitate reverse controlled antegrade and retrograde tracking techniques with ultrasound-guided relative wire-lumen-dissection spaces detection (18) (***Figure 4, panels C and D***). The importance of IVUS in PCI-guidance was shown by four meta-analyses, where this strategy was associated with reduced stent thrombosis, myocardial infarction (MI), repeat revascularization, and mortality (19-22). The largest and most recently published meta-analysis by Ahn

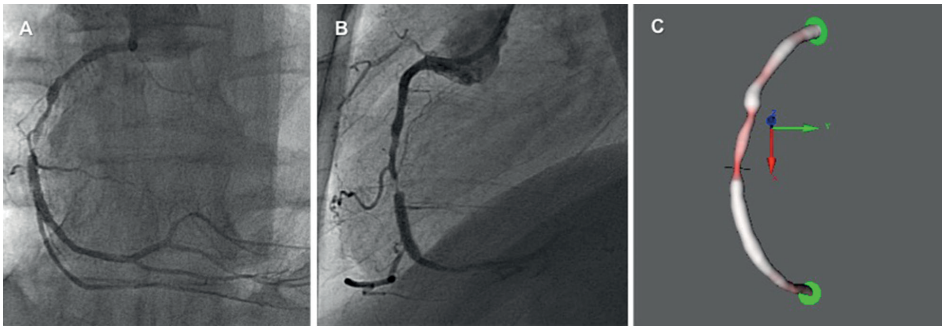

Figure 3. Example of 63-year-old patient with previous PCI of the right coronary artery and stable angina. The coronary angiogram (panels A and B) revealed a severe stenosis of the middle segment of the previously stented coronary artery. The two different angiographic projections have been used to three-dimensionally reconstruct the interested vessel-segment (panel C) with a dedicated 3D-QCA software using non-orthogonal angiographic projections. Increased stenosis severity is indicated by increasing darkness in red color.

3D-QCA: three-dimensional quantitative coronary angiography; PCI: percutaneous coronary intervention.

Note: Panel C is a modified edition of a figure published in Eurointervention by Pyxaras et al. (Eurointervention 2013; 9:889)

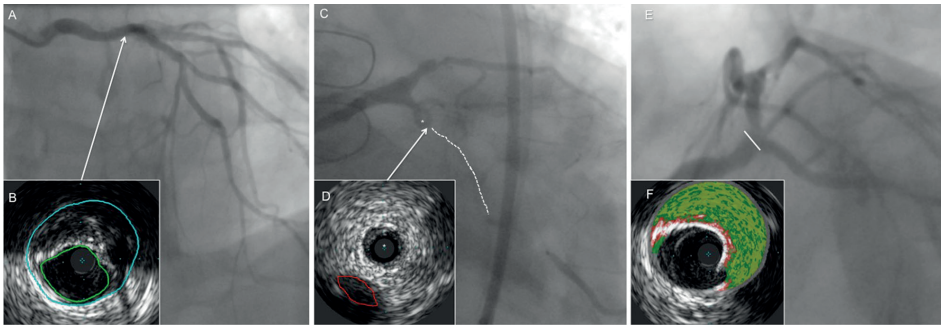

Figure 4. Use of IVUS and IVUS-VH.

Panel A: Coronary angiogram indicating a "tapered" left-main stenosis.

Panel B: The IVUS revealed a severe (area stenosis 70.9%, MLA 5.6 mm^2) calficied lesion at the distal lef-main, which was invisible to coronary angiography. The blue line indicates the reference vessel area, the green line shows the actual vessel lumen.

Panel C: Coronary angiogram - the left circumflex artery (here indicated by the white dotted line) is chronically occluded; an IVUS catheter is placed at a small side branch (indicated by asterisk) in front of the chronic total occlusion (CTO). *Panel D:* The IVUS shows the site of the lumen (highlighted by the red line) of the occluded left-circumflex artery.

Panel E: Coronary angiogram showing an intermediate severity distal left main stenosis; the white line corresponds to the cross-section of IVUS-VH shown in

Panel F: IVUS-VH identifying a heavily calcified eccentric atherosclerotic plaque (calcium shown in white), with elements of necrotic core (shown in red) and mixed composition of fibrous (dark green) and fibrofatty (light green) tissue.

CTO: chronic total occlusion; IVUS: intravascular ultrasound; IVUS-VH: intravascular ultrasound with virtual histology; MLA: minimal luminal area.

et al. included three randomized and 14 observational studies (total 26,503 patients), showing that IVUS-guided PCI as compared to angiography-guided PCI was consistent with risk of death, MI, target lesion revascularization (TLR), and stent thrombosis after drug-eluting stent implantation (22).

In addition, tissue characterization (fibrous tissue, fibro-fatty tissue, necrotic core and dense calcium) of coronary vessels is feasible using virtual histology intravascular ultrasound (VH-IVUS), an imaging modality based upon the spectral analysis of the primary raw backscattered ultrasound wave [radiofrequency (RF)-based signal] (***Figure 4, panels E and F***). Findings such as a large necrotic core, thin-cap fibro-atheroma (TCFA) and the presence of plaque rupture, were associated with peri-procedural MI during stent implantation (23). The PROSPECT trial showed that in patients who presented with an acute coronary syndrome and underwent PCI, major adverse cardiovascular events occurring during three years of follow-up were equally attributable to recurrence at the site of culprit lesions and to non-culprit lesions (24). In this setting, VH-IVUS-identified TCFAs in non-culprit lesions, as well as plaque burden >70% and MLA <4.0 mm^2, emerged as independent predictors of MACE. These findings suggest a possible role of VH-IVUS to potentially identify vulnerable plaques, as integral part of primary or secondary prevention. This hypothesis is further supported by the VIVA and ATHEROREMO-IVUS trials, showing that optimal medical therapy may have an impact on revascularization rates (25,26). Serruys et al. showed that lipoprotein-associated phospholipase A_2 – Inhibition with Darapladib prevented the expansion of necrotic core in coronary lesions; these findings may suggest a possible role of this drug on reducing plaque vulnerability (27).

Optical coherence tomography (OCT)

Optical coherence tomography was developed as an intravascular imaging modality that uses light transmission properties. Cross-sectional images are generated by measuring the echo time delay and intensity of light that is reflected or backscattered from internal structures in tissue. The axial resolution, determined by the light wavelength, ranges from 12 to 18 µm, compared with 150 to 200 µm for IVUS. Due to this unmatched high resolution, OCT can provide in-cathlab – in-vivo histology imaging of the epicardial vessels. Accordingly, it allows (i) precise tissue characterization (***Figure 5, panels A, B, C and D***); and (ii) stent strut-level description (***Figure 5, panels E and F***). Both features are of fundamental importance for pathophysiologic on-site diagnosis and PCI-guidance. First, OCT accurately visualizes coronary tissue composition, enabling qualitative and quantitative assessment of calcifications (2), lipid pools (28), intracoronary white and red thrombus (29), thin- and thick-cap fibro-atheroma (30). The abovementioned characteristic features render OCT a unique diagnostic opportunity of direct visualization and description of vulnerable plaques, defined as coronary atherosclerotic plaques prone to rupture and, as such, at high risk of producing acute coronary thrombosis and subsequent MI. Recently, Uemura et al. showed that

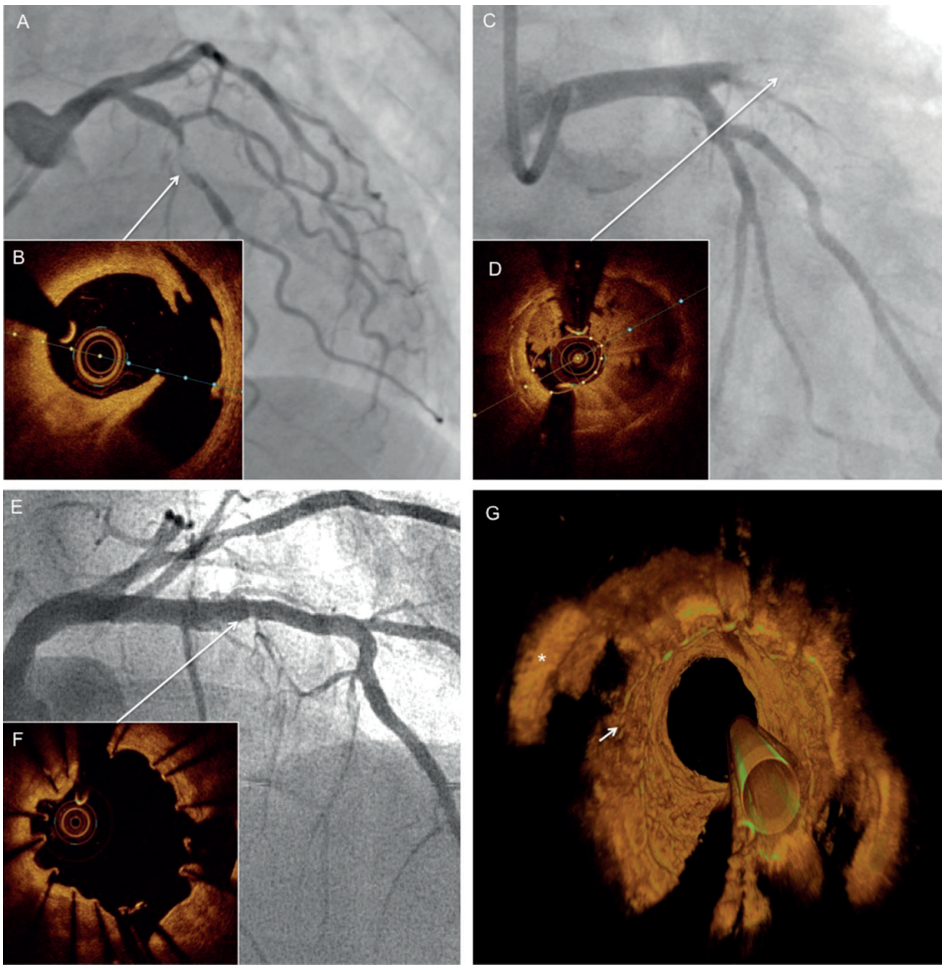

Figure 5. OCT imaging.
Panel A shows a coronary angiogram with a suboclusive mid-LAD Stenosis, OCT-analysis identifies an extended dissection (*panel B*). The coronary angiogram of *Panel C* demonstrates an occluded stent in the proximal LAD; OCT shows in-stent thrombosis (Panel D), responsible for the vessel occlusion. The coronary angiogram of *Panel E* is at first glance unremarkable, however OCT reveals a massive stent-malapposition of a previously implanted drug-eluting stent (panel F); *Panel G* shows the 3D-OCT of this latter (the asterisk corresponds to the vessel wall, which is at a consdirable distance from the stent struts, here indicated by arrow).
LAD: left anterior descending artery; OCT: optical coherence tomography; 3D-OCT: three-dimensional optical coherence tomography.

OCT-identified TCFAs in 53 consecutive CAD patients predict progression of non-obstructive coronary plaques (31). Furthermore, Tian et al. identified a fibrous cap thickness <52 µm as a critical morphological discriminator between ruptured plaques and non-ruptured TCFAs (32).

OCT's ability to assess luminal areas and identify underexpansion, malapposition, stent-edge dissection provides an invaluable tool of PCI-optimization. The retrospective CLI-OPCI study

reported that angiography plus OCT guidance versus angiography-only guidance for PCI was associated with a significantly lower risk of cardiac death or MI at 1 year (33). OCT-based device assessment has been extensively used to assess efficacy and safety of bioresorbable scaffolds. Analyses of the ABSORB-cohort B patient population showed that OCT-diagnosed baseline scaffold malapposition is associated to uncovered struts and intracoronary masses at 6 months of follow-up (34). Likewise, Mattesini et al. used systematically OCT-guidance as an integrative part of coronary bioresorbable scaffold implantation, a strategy that guaranteed a safety profile comparable to 2nd generation DES (35). Recently, presented data from the ILUMIEN I study showed that OCT imaging performed before and after PCI is capable of conditioning operators' clinical judgment in 65% of cases and is associated with reduced rates of MI (36). The ILUMIEN II study data suggest that OCT guidance offers rates of stent expansion similar to IVUS-guidance (37).

The latest advances in OCT technology permit high-speed acquisitions up to 160 frames/s during the pullback, which allows three-dimensional vessel reconstructions of unprecedented detail (***Figure 5, panel G***) (38). Okamura et al. recently showed the feasibility of 3D-OCT reconstructions after bioresorbable scaffold implantation, allowing the evaluation of jailed side branches in the setting of bifurcation lesion treatment (39). The same technique has been successfully used to confirm optimal side-branch re-wiring in PCI with DES, reducing significantly the rate of incomplete stent apposition (40). Larger studies and randomized trials are warranted to address the potential clinical impact of the use of OCT and 3D-OCT.

FUNCTIONAL ASSESSMENT

Fractional Flow Reserve (FFR)

Fractional flow reserve (FFR) has been introduced by Pijls et al. as the ratio between intracoronary pressure (Pd) (assessed distally to a given stenosis) and aortic pressure (Pa), during maximal hyperemia (41):

$$FFR = \frac{Pd}{Pa}$$

This simplified equation reflects the ratio of hyperemic myocardial flow in the stenotic territory ($Q_S max$) to normal hyperemic myocardial flow ($Q_N max$), since, under maximal hyperemia, resistances are minimal and therefore waived:

$$FFR = \frac{Qsmax}{QNmax}$$

or, equally,

$$FFR = \frac{(Pd - Pv)/Rsmax}{(Pa - Pv)/RNmax}$$

where $R_S$max and $R_N$max are, respectively, the hyperemic myocardial resistance in the stenotic territory and hyperemic myocardial resistance in the normal territory, and Pv the venous pressure. When the resistances under maximal hyperemia are waived:

$$FFR = \frac{Pd - Pv}{Pa - Pv}$$

Considering Pv as negligible,

$$FFR = \frac{Pd}{Pa}$$

The cut-off FFR value currently in use, as validated in extended clinical studies and suggested by current guidelines, is 0.80 (threshold of abnormality) (3,4,42).

Fractional flow reserve measurements can be routinely performed during a heart catheterization procedure to guide clinical decision making on-site. Commercially available a 0.014-inch miniaturized pressure wires are introduced in the coronary artery through conventional guiding catheters. After equalization of the Pa and Pd, the wire is advanced and positioned distally to the coronary stenosis. Maximal hyperemia is achieved usually with adenosine, administrated intravenously at 140 μg/kg/min or intracoronary, using boluses of 40 μg for the right and 80 μg for the left coronary artery. A recent study by Adjedj et al. showed that intracoronary administration of adenosine gives identical FFR values compared to intravenous administration (43). Abrupt Pd-variations during wire pullback are synonym of focalized hemodynamically significant stenoses, while gradual, homogeneous variations of intracoronary pressures indicate diffuse atherosclerotic disease.

In the setting of stable ischemic heart disease, a diagnostic-therapeutic strategy that integrates FFR in its algorithm has a proven superiority in terms of clinical outcome as compared to angiography alone. The long-term results of the DEFER study show that medical treatment is safe in patients without FFR-assessed myocardial ischemia (44). The FAME trial demonstrated that patients with multi-vessel disease benefit from FFR-guided PCI with respect to the composite end-point of death, MI and repeat revascularization (4). Furthermore, findings from the FAME-2 study show that FFR-guided PCI reduces significantly the need for repeat revascularization in patients with stable CAD (3). Accordingly, FFR assessment is highly recommended for patients without previous non-invasive assessment of ischemia (5). Furthermore, retrospective data suggest that FFR-guided coronary artery bypass surgery may be associated with a lower number of graft anastomoses and lower rate of on-pump surgery compared with conventional, angiography-guided bypass surgery (45), however this concept remains to be confirmed by large scale randomized trials. Likewise, Layland et al. suggested that FFR may have a role in guiding PCI in patients with acute coronary syndrome (46), since FFR guidance modified the operator's decision in approximately 20% of cases; no differences in clinical outcome were detected although the study was underpowered for the secondary, clinical end-point.

Index of Microvascular Resistance

The index of microvascular resistance (IMR) is defined as the mean distal pressure multiplied by the mean hyperemic transit time:

$$IMR = \frac{Pd - Pv}{1/Tm},$$

where Pd is the distal coronary pressure, Pv the venous pressure and Tm the mean hyperemic transit time. According to the assumption already made for the FFR estimation that Pv is negligible, the above equation can be equally written

$$IMR = \frac{Pd}{1/Tm},$$

or

$$IMR = Pd \times Tm.$$

IMR is derived from the assumption that minimum microvascular resistance is achieved at maximum hyperemia, due to the elimination of the variability of resting vascular tone and hemodynamics (47).

Measurement of IMR is performed during maximal, steady-state hyperemia induced by infusing intravenous adenosine at 140 µg/kg/min. The coronary pressure wire is calibrated, equalized to the guide catheter pressure with the pressure wire sensor positioned at the tip of the catheter, and then advanced to the distal two-thirds of the coronary artery. Three milliliters of room temperature saline are briskly injected through the guide catheter, and Tm is measured by using the thermodilution technique (48,49). Three different measurements are usually performed and averaged. In parallel, Pd is measured with the pressure wire.

IMR is a readily available tool of microvascular resistance measurements in the cathlab and implies the possibility of simultaneous FFR assessment. In addition, its value is not affected by the epicardial stenosis severity (50). While FFR specifically assess the epicardial-vessel conductance and is independent of microvasculature status, IMR reflects the coronary microvascular

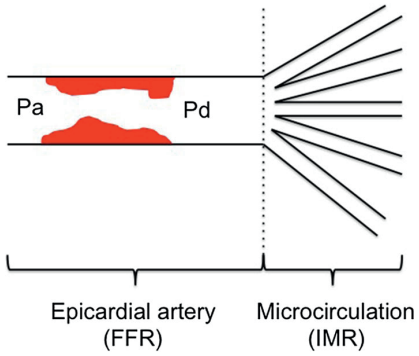

Figure 6. Schematic representation of physiology-derived metrics used for the functional assessment of coronary artery disease in the catheterization laboratory. Fractional flow reserve (FFR) measures the epicardial vessel pressure-drop, reflecting the epicardial vessel conductance, independently from the microvasculature. The index of microvasculature resistance (IMR) assesses instead the coronary microcirculation. Both metrics are assessed during conditions of maximal hyperemia.
FFR: fractional flow reserve; IMR: index of microvasculature resistance; Pa: aortic pressure; Pd: intracoronary pressure.

conditions (**Figure 6**). These characteristics offer the possibility of an integrated physiologic approach during the same catheterization laboratory session, enhancing the quantity of information retrieved, with potential impact on final decision-making regarding treatment (PCI vs. medical treatment).

Fearon et al. showed that IMR has a prognostic value when assessed immediately after primary PCI (51). In a series of 253 patients, an elevated IMR value (>40) measured after primary PCI emerged as independent predictor of death or re-hospitalization for heart failure. Cuculi et al. demonstrated that IMR values evolve in patients undergoing primary PCI, showing a significant reduction, both 24 hours after MI and at 6 months follow-up (52). A larger randomized trial is warranted to confirm the role of IMR in prognostic stratification of patients with ischemic heart disease.

Non-hyperemic physiologic indexes

During the past few years, an effort has been made to develop novel physiologic indexes that would be independent of conditions of maximal hyperemia. Sen et al. developed the instantaneous wave-free reserve (iFR), using an integrated algorithm to estimate Pd/Pa value during the wave-free period (defined as the time-frame of end-diastole (53). This method showed good correlation on predicting FFR, in particular for angiographically severe or low-grade stenoses (54). The "Multicenter Core Laboratory Comparison of the Instantaneous Wave-Free Ratio and Resting Pd/Pa With Fractional Flow Reserve" (RESOLVE) study showed a good correlation of both iFR and Pd/Pa with FFR values (55). Recently, two randomized trials in large patient populations were performed to investigate the role of iFR in the prognostic stratification of patients with CAD. The DEFINE-FLAIR (Functional Lesion Assessment of Intermediate Stenosis to Guide Revascularisation) study randomized 2492 patients with CAD to undergo either iFR-guided or FFR-guided coronary revascularization. At 1 year of follow-up, iFR-guided revascularization showed non-inferiority as with respect to FFR-guided-PCI for the composite end-point of death from any cause, nonfatal myocardial infarction, or unplanned revascularization (major adverse cardiac events – MACE). Furthermore, the number of patients who had adverse procedural symptoms and clinical signs was significantly lower in the iFR group than in the FFR group (56). Likewise, the Instantaneous Wave-free Ratio versus Fractional Flow Reserve in Patients with Stable Angina Pectoris or Acute Coronary Syndrome (iFR-SWEDEHEART) study randomized 2037 patients with stable angina or an acute coronary syndrome to iFR- or FFR-guided-PCI. At 1 year of follow-up, the MACE rate was not significantly different between the two patient subgroups (57).

Intracoronary contrast-medium administration is under investigation as agent of "partial" hyperemia. The Rapid injection of contrast medium vs. nitroprusside or adenosine in intermediate coronary Stenoses" (RINASCI) study showed a satisfactory correlation of "contrast-induced FFR" with FFR values (58). Tu et al. recently introduced new software capable of estimating FFR based on an algorithm assessing the TIMI frame-count (59).

CORRELATION BETWEEN ANATOMICAL AND FUNCTIONAL METRICS

Several studies sought to identify the possible correlation between anatomic findings and physiologic indexes, being both approaches readily available during heart catheterization procedures.

Traditionally, diagnostic assessment of coronary artery disease has been based on a qualitative (visual) angiographic threshold of 50% of diameter stenosis (DS) (60), this latter based on animal experiments showing a decline in hyperemic myocardial flow reserve below 4.0 for DS >50% (61). However, this approach is limited by an oversimplified assessment of stenosis severity. Indeed, Nallamothu et al. showed that in a series of 216 lesions treated with PCI, the mean difference between qualitative assessment and QCA was 8.2±8.4% ($p<0.001$), reflecting the clinical overestimation of a given stenosis (8). Differences were even higher for intermediate (i.e. ranging between 50-70% as assessed by QCA) coronary stenoses (mean difference 12.3±8.4%).

Despite the inherent limits of qualitative assessment of the coronary angiogram, QCA itself did not manage to improve diagnostic accuracy on predicting the functional significance of coronary stenoses. In a large retrospective cohort of 4086 stenoses assessed with QCA and FFR, Toth et al. observed discordance between QCA-assessed DS and FFR in one third of cases (62). The diagnostic accuracy of a 50%DS cut-off for predicting FFR <0.80 was 64%. Interestingly, findings by Fischer et al. suggest that the combination of DS and minimal luminal diameter (MLD) might confer more precision to angiography: all patients with QCA-derived DS <60% or MLD>1.4 mm had all FFR>0.75 (63). However, also in this study, QCA metrics were not able to discriminate lesion significance outside of these parameters.

Recently, the diagnostic accuracy of 3D-QCA on predicting FFR as an alternative to conventional QCA was assessed. Yong et al. performed 2D-QCA, 3D-QCA and FFR in 63 lesions and found that the most accurate predictor of FFR <0.75 was MLA assessed by 3D-QCA ($R=0.63$, $p<0.001$) (64). Saad et al. assessed 41 intermediate coronary lesions and showed a significant correlation between cross-sectional stenosis and FFR <0.75 ($r=-0.481$, $p=0.001$) (65). In a retrospective series of 55 non-obstructive coronary stenoses, our group documented a significant correlation between 3D-QCA-derived MLA and FFR ($R^2=0.47$, $p<0.001$) (11). Although the abovementioned findings are limited to relatively small patient-lesion samples, they suggest that 3D-QCA may be of use on assessing the functional significance of lesions when FFR is not available or contraindicated.

Historically, first attempts of correlation between intravascular imaging – derived metrics and functional assessment in the cathlab have been performed using intravascular ultrasound (IVUS). Takagi et al. assessed 51 lesions in 42 patients with IVUS and FFR and found that a minimum luminal area (MLA) of 3.0 mm^2 had 88% accuracy on predicting FFR $\leq$0.75 (66). In 55 patients with angiographically ambiguous LM stenosis, Jasti et al. compared IVUS-derived minimum luminal diameter (MLD) and minimum luminal area (MLA) with FFR (gold

standard), finding that an IVUS MLD and MLA of 2.8 mm and 5.9 mm^2 predict FFR ≤0.75 (17). The lack of randomized data for both FFR and IVUS in the setting of LM stenosis suggest the complementary use of IVUS in clinical practice for FFR values varying between 0.80 and 0.85 (67).

Despite its unprecedented detail of image acquisition, OCT failed to show superior results with respect to IVUS on predicting FFR. Gonzalo et al. showed that among 61 stenoses (56 patients) with a mean FFR of 0.80±0.11, minimal luminal diameter assessed by OCT had a moderate diagnostic accuracy of 73% on predicting FFR values ≤0.80 (68). Shiono et al. found a better diagnostic accuracy (85.5%) of OCT-derived minimal luminal diameter, however the mean FFR values in 62 coronary stenoses were significantly lower (0.72±0.14) with respect to Gonzalo et al. (69). We showed an accuracy of OCT-derived minimal luminal diameter of 80%, when mean FFR was 0.85±0.10 (55 stenoses assessed) (11). These findings suggest that the correlation between OCT and FFR is rather weak, particularly for coronary stenoses with FFR values that move around the cut-off limit of 0.80. Accordingly, OCT cannot be intended as a potential surrogate of FFR for the functional assessment of coronary stenoses.

Conclusion

Current evidence suggests that invasive diagnostic assessment during a cathlab session offers extremely useful information, not only to help on-site decision-making, but also to guide the interventional strategy. Fractional flow reserve has a gatekeeper role on indicating adequacy of intervention. On the other hand, intravascular imaging can be used for procedural optimization, offering invaluable insights for lesion characterization and stent deployment. An integrated anatomic-physiologic approach seems to be the best option for the individual patient in order to maximize procedural and clinical outcome.

REFERENCES

1. Mintz GS, Weissman NJ. Intravascular ultrasound in the drug-eluting stent era. J Am Coll Cardiol 2006;48:421-9.
2. Tearney GJ, Regar E, Akasaka T et al. Consensus standards for acquisition, measurement, and reporting of intravascular optical coherence tomography studies: a report from the International Working Group for Intravascular Optical Coherence Tomography Standardization and Validation. J Am Coll Cardiol 2012;59:1058-72.
3. De Bruyne B, Pijls NH, Kalesan B et al. Fractional flow reserve-guided PCI versus medical therapy in stable coronary disease. N Engl J Med 2012;367:991-1001.
4. Tonino PA, De Bruyne B, Pijls NH et al. Fractional flow reserve versus angiography for guiding percutaneous coronary intervention. N Engl J Med 2009;360:213-24.
5. Kolh P, Windecker S, Alfonso F et al. 2014 ESC/EACTS Guidelines on myocardial revascularization: the Task Force on Myocardial Revascularization of the European Society of Cardiology (ESC) and the European Association for Cardio-Thoracic Surgery (EACTS). Developed with the special contribution of the European Association of Percutaneous Cardiovascular Interventions (EAPCI). Eur J Cardiothorac Surg 2014;46:517-92.
6. Stadius ML, Alderman EL. Coronary artery revascularization. Critical need for, and consequences of, objective angiographic assessment of lesion severity. Circulation 1990;82:2231-4.
7. Berry C, L'Allier PL, Gregoire J et al. Comparison of intravascular ultrasound and quantitative coronary angiography for the assessment of coronary artery disease progression. Circulation 2007;115:1851-7.
8. Nallamothu BK, Spertus JA, Lansky AJ et al. Comparison of clinical interpretation with visual assessment and quantitative coronary angiography in patients undergoing percutaneous coronary intervention in contemporary practice: the Assessing Angiography (A2) project. Circulation 2013;127:1793-800.
9. Grundeken MJ, Ishibashi Y, Ramcharitar S et al. The need for dedicated bifurcation quantitative coronary angiography (QCA) software algorithms to evaluate bifurcation lesions. EuroIntervention 2015;11 Suppl V:V44-9.
10. Grundeken MJ, Ishibashi Y, Genereux P et al. Inter-core lab variability in analyzing quantitative coronary angiography for bifurcation lesions: a post-hoc analysis of a randomized trial. JACC Cardiovasc Interv 2015;8:305-14.
11. Pyxaras SA, Tu S, Barbato E et al. Quantitative angiography and optical coherence tomography for the functional assessment of nonobstructive coronary stenoses: comparison with fractional flow reserve. Am Heart J 2013;166:1010-1018 e1.
12. Sanidas E, Dangas G. Evolution of intravascular assessment of coronary anatomy and physiology: from ultrasound imaging to optical and flow assessment. Eur J Clin Invest 2013;43:996-1008.
13. Mintz GS. Clinical utility of intravascular imaging and physiology in coronary artery disease. J Am Coll Cardiol 2014;64:207-22.
14. Oviedo C, Maehara A, Mintz GS et al. Intravascular ultrasound classification of plaque distribution in left main coronary artery bifurcations: where is the plaque really located? Circ Cardiovasc Interv 2010;3:105-12.
15. de la Torre Hernandez JM, Hernandez Hernandez F, Alfonso F et al. Prospective application of pre-defined intravascular ultrasound criteria for assessment of intermediate left main coronary artery lesions results from the multicenter LITRO study. J Am Coll Cardiol 2011;58:351-8.

16. Hamilos M, Muller O, Cuisset T et al. Long-term clinical outcome after fractional flow reserve-guided treatment in patients with angiographically equivocal left main coronary artery stenosis. Circulation 2009;120:1505-12.
17. Jasti V, Ivan E, Yalamanchili V, Wongpraparut N, Leesar MA. Correlations between fractional flow reserve and intravascular ultrasound in patients with an ambiguous left main coronary artery stenosis. Circulation 2004;110:2831-6.
18. Rathore S, Katoh O, Tuschikane E, Oida A, Suzuki T, Takase S. A novel modification of the retrograde approach for the recanalization of chronic total occlusion of the coronary arteries intravascular ultrasound-guided reverse controlled antegrade and retrograde tracking. JACC Cardiovasc Interv 2010;3:155-64.
19. Zhang Y, Farooq V, Garcia-Garcia HM et al. Comparison of intravascular ultrasound versus angiography-guided drug-eluting stent implantation: a meta-analysis of one randomised trial and ten observational studies involving 19,619 patients. EuroIntervention 2012;8:855-65.
20. Klersy C, Ferlini M, Raisaro A et al. Use of IVUS guided coronary stenting with drug eluting stent: a systematic review and meta-analysis of randomized controlled clinical trials and high quality observational studies. Int J Cardiol 2013;170:54-63.
21. Jang JS, Song YJ, Kang W et al. Intravascular ultrasound-guided implantation of drug-eluting stents to improve outcome: a meta-analysis. JACC Cardiovasc Interv 2014;7:233-43.
22. Ahn JM, Kang SJ, Yoon SH et al. Meta-analysis of outcomes after intravascular ultrasound-guided versus angiography-guided drug-eluting stent implantation in 26,503 patients enrolled in three randomized trials and 14 observational studies. Am J Cardiol 2014;113:1338-47.
23. Claessen BE, Maehara A, Fahy M, Xu K, Stone GW, Mintz GS. Plaque composition by intravascular ultrasound and distal embolization after percutaneous coronary intervention. JACC Cardiovasc Imaging 2012;5:S111-8.
24. Stone GW, Maehara A, Lansky AJ et al. A prospective natural-history study of coronary atherosclerosis. N Engl J Med 2011;364:226-35.
25. Calvert PA, Obaid DR, O'Sullivan M et al. Association between IVUS findings and adverse outcomes in patients with coronary artery disease: the VIVA (VH-IVUS in Vulnerable Atherosclerosis) Study. JACC Cardiovasc Imaging 2011;4:894-901.
26. Cheng JM, Garcia-Garcia HM, de Boer SP et al. In vivo detection of high-risk coronary plaques by radiofrequency intravascular ultrasound and cardiovascular outcome: results of the ATHEROREMO-IVUS study. Eur Heart J 2014;35:639-47.
27. Serruys PW, Garcia-Garcia HM, Buszman P et al. Effects of the direct lipoprotein-associated phospholipase A(2) inhibitor darapladib on human coronary atherosclerotic plaque. Circulation 2008;118:1172-82.
28. Prati F, Guagliumi G, Mintz GS et al. Expert review document part 2: methodology, terminology and clinical applications of optical coherence tomography for the assessment of interventional procedures. Eur Heart J 2012;33:2513-20.
29. Onuma Y, Thuesen L, van Geuns RJ et al. Randomized study to assess the effect of thrombus aspiration on flow area in patients with ST-elevation myocardial infarction: an optical frequency domain imaging study--TROFI trial. Eur Heart J 2013;34:1050-60.
30. Sinclair H, Bourantas C, Bagnall A, Mintz GS, Kunadian V. OCT for the identification of vulnerable plaque in acute coronary syndrome. JACC Cardiovasc Imaging 2015;8:198-209.
31. Uemura S, Ishigami K, Soeda T et al. Thin-cap fibroatheroma and microchannel findings in optical coherence tomography correlate with subsequent progression of coronary atheromatous plaques. Eur Heart J 2012;33:78-85.

32. Tian J, Ren X, Vergallo R et al. Distinct morphological features of ruptured culprit plaque for acute coronary events compared to those with silent rupture and thin-cap fibroatheroma: a combined optical coherence tomography and intravascular ultrasound study. J Am Coll Cardiol 2014;63:2209-16.
33. Prati F, Di Vito L, Biondi-Zoccai G et al. Angiography alone versus angiography plus optical coherence tomography to guide decision-making during percutaneous coronary intervention: the Centro per la Lotta contro l'Infarto-Optimisation of Percutaneous Coronary Intervention (CLI-OPCI) study. EuroIntervention 2012;8:823-9.
34. Gomez-Lara J, Radu M, Brugaletta S et al. Serial analysis of the malapposed and uncovered struts of the new generation of everolimus-eluting bioresorbable scaffold with optical coherence tomography. JACC Cardiovasc Interv 2011;4:992-1001.
35. Mattesini A, Secco GG, Dall'Ara G et al. ABSORB biodegradable stents versus second-generation metal stents: a comparison study of 100 complex lesions treated under OCT guidance. JACC Cardiovasc Interv 2014;7:741-50.
36. Wijns W, Shite J, Jones MR et al. Optical coherence tomography imaging during percutaneous coronary intervention impacts physician decision-making: ILUMIEN I study. Eur Heart J 2015;36:3346-55.
37. Maehara A, Ben-Yehuda O, Ali Z et al. Comparison of Stent Expansion Guided by Optical Coherence Tomography Versus Intravascular Ultrasound: The ILUMIEN II Study (Observational Study of Optical Coherence Tomography [OCT] in Patients Undergoing Fractional Flow Reserve [FFR] and Percutaneous Coronary Intervention). JACC Cardiovasc Interv 2015;8:1704-14.
38. Farooq V, Gogas BD, Okamura T et al. Three-dimensional optical frequency domain imaging in conventional percutaneous coronary intervention: the potential for clinical application. Eur Heart J 2013;34:875-85.
39. Okamura T, Onuma Y, Garcia-Garcia HM et al. 3-Dimensional optical coherence tomography assessment of jailed side branches by bioresorbable vascular scaffolds: a proposal for classification. JACC Cardiovasc Interv 2010;3:836-44.
40. Okamura T, Onuma Y, Yamada J et al. 3D optical coherence tomography: new insights into the process of optimal rewiring of side branches during bifurcational stenting. EuroIntervention 2014;10:907-15.
41. Pijls NH, van Son JA, Kirkeeide RL, De Bruyne B, Gould KL. Experimental basis of determining maximum coronary, myocardial, and collateral blood flow by pressure measurements for assessing functional stenosis severity before and after percutaneous transluminal coronary angioplasty. Circulation 1993;87:1354-67.
42. Task Force on Myocardial Revascularization of the European Society of C, the European Association for Cardio-Thoracic S, European Association for Percutaneous Cardiovascular I et al. Guidelines on myocardial revascularization. Eur Heart J 2010;31:2501-55.
43. Adjedj J, Toth GG, Johnson NP et al. Intracoronary Adenosine: Dose-Response Relationship With Hyperemia. JACC Cardiovasc Interv 2015;8:1422-30.
44. Pijls NH, van Schaardenburgh P, Manoharan G et al. Percutaneous coronary intervention of functionally nonsignificant stenosis: 5-year follow-up of the DEFER Study. J Am Coll Cardiol 2007;49:2105-11.
45. Toth G, De Bruyne B, Casselman F et al. Fractional flow reserve-guided versus angiography-guided coronary artery bypass graft surgery. Circulation 2013;128:1405-11.

46. Layland J, Oldroyd KG, Curzen N et al. Fractional flow reserve vs. angiography in guiding management to optimize outcomes in non-ST-segment elevation myocardial infarction: the British Heart Foundation FAMOUS-NSTEMI randomized trial. Eur Heart J 2015;36:100-11.
47. Fearon WF, Balsam LB, Farouque HM et al. Novel index for invasively assessing the coronary microcirculation. Circulation 2003;107:3129-32.
48. De Bruyne B, Pijls NH, Smith L, Wievegg M, Heyndrickx GR. Coronary thermodilution to assess flow reserve: experimental validation. Circulation 2001;104:2003-6.
49. Pijls NH, De Bruyne B, Smith L et al. Coronary thermodilution to assess flow reserve: validation in humans. Circulation 2002;105:2482-6.
50. Aarnoudse W, Fearon WF, Manoharan G et al. Epicardial stenosis severity does not affect minimal microcirculatory resistance. Circulation 2004;110:2137-42.
51. Fearon WF, Low AF, Yong AS et al. Prognostic value of the Index of Microcirculatory Resistance measured after primary percutaneous coronary intervention. Circulation 2013;127:2436-41.
52. Cuculi F, De Maria GL, Meier P et al. Impact of microvascular obstruction on the assessment of coronary flow reserve, index of microcirculatory resistance, and fractional flow reserve after ST-segment elevation myocardial infarction. J Am Coll Cardiol 2014;64:1894-904.
53. Sen S, Escaned J, Malik IS et al. Development and validation of a new adenosine-independent index of stenosis severity from coronary wave-intensity analysis: results of the ADVISE (ADenosine Vasodilator Independent Stenosis Evaluation) study. J Am Coll Cardiol 2012;59:1392-402.
54. Berry C, van 't Veer M, Witt N et al. VERIFY (VERification of Instantaneous Wave-Free Ratio and Fractional Flow Reserve for the Assessment of Coronary Artery Stenosis Severity in EverydaY Practice): a multicenter study in consecutive patients. J Am Coll Cardiol 2013;61:1421-7.
55. Jeremias A, Maehara A, Genereux P et al. Multicenter core laboratory comparison of the instantaneous wave-free ratio and resting Pd/Pa with fractional flow reserve: the RESOLVE study. J Am Coll Cardiol 2014;63:1253-61.
56. Davies JE, Sen S, Dehbi HM et al. Use of the Instantaneous Wave-free Ratio or Fractional Flow Reserve in PCI. N Engl J Med 2017;376:1824-1834.
57. Gotberg M, Christiansen EH, Gudmundsdottir IJ et al. Instantaneous Wave-free Ratio versus Fractional Flow Reserve to Guide PCI. N Engl J Med 2017;376:1813-1823.
58. Leone AM, Scalone G, De Maria GL et al. Efficacy of contrast medium induced Pd/Pa ratio in predicting functional significance of intermediate coronary artery stenosis assessed by fractional flow reserve: insights from the RINASCI study. EuroIntervention 2015;11:421-7.
59. Tu S, Barbato E, Koszegi Z et al. Fractional flow reserve calculation from 3-dimensional quantitative coronary angiography and TIMI frame count: a fast computer model to quantify the functional significance of moderately obstructed coronary arteries. JACC Cardiovasc Interv 2014;7:768-77.
60. Task Force M, Montalescot G, Sechtem U et al. 2013 ESC guidelines on the management of stable coronary artery disease: the Task Force on the management of stable coronary artery disease of the European Society of Cardiology. Eur Heart J 2013;34:2949-3003.
61. Gould KL, Lipscomb K. Effects of coronary stenoses on coronary flow reserve and resistance. Am J Cardiol 1974;34:48-55.
62. Toth G, Hamilos M, Pyxaras S et al. Evolving concepts of angiogram: fractional flow reserve discordances in 4000 coronary stenoses. Eur Heart J 2014;35:2831-8.
63. Fischer JJ, Samady H, McPherson JA et al. Comparison between visual assessment and quantitative angiography versus fractional flow reserve for native coronary narrowings of moderate severity. Am J Cardiol 2002;90:210-5.

64. Yong AS, Ng AC, Brieger D, Lowe HC, Ng MK, Kritharides L. Three-dimensional and two-dimensional quantitative coronary angiography, and their prediction of reduced fractional flow reserve. Eur Heart J 2011;32:345-53.
65. Saad M, Toelg R, Khattab AA, Kassner G, Abdel-Wahab M, Richardt G. Determination of haemodynamic significance of intermediate coronary lesions using three-dimensional coronary reconstruction. EuroIntervention 2009;5:573-9.
66. Takagi A, Tsurumi Y, Ishii Y, Suzuki K, Kawana M, Kasanuki H. Clinical potential of intravascular ultrasound for physiological assessment of coronary stenosis: relationship between quantitative ultrasound tomography and pressure-derived fractional flow reserve. Circulation 1999;100:250-5.
67. Puri R, Kapadia SR, Nicholls SJ, Harvey JE, Kataoka Y, Tuzcu EM. Optimizing outcomes during left main percutaneous coronary intervention with intravascular ultrasound and fractional flow reserve: the current state of evidence. JACC Cardiovasc Interv 2012;5:697-707.
68. Gonzalo N, Escaned J, Alfonso F et al. Morphometric assessment of coronary stenosis relevance with optical coherence tomography: a comparison with fractional flow reserve and intravascular ultrasound. J Am Coll Cardiol 2012;59:1080-9.
69. Shiono Y, Kitabata H, Kubo T et al. Optical coherence tomography-derived anatomical criteria for functionally significant coronary stenosis assessed by fractional flow reserve. Circ J 2012;76:2218-25.